Comparing retrieved optical depth from a high-order model and a zero-order model and analyzing their relationship with vegetation properties

Somayeh Talebiesfandarani

Iranian Space Research Center, Tehran, Iran – so.talebi@gmail.com, s.talebi@isrc.ac.ir

Keyword: High-order model, Zero-order model, Optical depth, Wheat

Abstract

Optical depth is significant key vegetation parameters in the study of vegetation canopy. Until now efforts have been made to estimate optical depth by fitting sensors brightness temperature to a zero-order model (τ-ω model). The τ-ω model is a simple model without considering multi-scattering effects inside the vegetation layer. Here effective optical depth (VODs) calculated from a high order model to take in to account multi-scattering effects. The high order model is a close simulation of the real situation. It enables investigating optical depth behavior during wheat grow season in different frequencies, incident angels and polarizations. Measured LAI, VWC and biomass were used to validate simulated VODs. VODs was corresponding to the measured vegetation parameters in terms of the trend and the time of maximum and the minimum values. Furthermore, equivalent optical depth (EVOD) was calculated by fitting brightness temperature to the zero-order model and compared with the VODs. Results indicated EVOD as VODs also were frequency, incident angle and polarization dependent but overestimated compare to VODs. Calculating optical depth of other types of vegetation with different structure can give more detailed in vegetation behavior during growing season.

1. Introduction

Vegetation, as a significant aspect of the ecosystem, has been widely studied in terms of monitoring its properties such as biomass, water content and coverage. Optical depth is significant key parameter in the study of vegetation canopy(Baur et al. 2019). Microwave attenuation properties of vegetation canopy can be explained by optical depth. Temporal optical depth is an effective parameter in monitoring biomass, VWC, crop water stress, global change monitoring, vegetation phenology, and drought(Jones et al. 2011; Liu et al. 2011; Guan et al. 2013; Guan et al. 2014; Ulaby et al. 2014). Radiative transfer models (RTM) are common to calculate optical depth and scattering albedo (Shi et al. 2008). High order models and zero order models are two types of RTM models. A high order model is a close simulation of the real situation by considering multi scattering effects insider the vegetation that enabled us to investigate optical depth and scattering albedo behavior in different frequencies, incident angels and polarizations during the vegetation growing season. The zero-order model (τ-ω model) is a simple radiative transfer model that simulates brightness temperature as a function of optical depth, single scattering albedo and soil emissivity. This model doesn't consider multi-scattering effects in the vegetation layer (Ferrazzoli et al. 2002). Nowadays in the microwave region of electromagnetic spectrum, the *τ-ω* inverse model from soil and vegetation layers is widely used to calculate soil moisture and optical depth for when scattering albedo was either eliminated or had a constant value(Jackson, 1993; Owe et al. 2001; Kerr et al. 2012; O'Neill et al. 2018; Gao et al. 2020). Techniques like the Single Channel Algorithm (SCA) (Jackson, 1993), The Dual Channel Algorithm (DCA) (O'Neill et al., 2018), Land Parameter Retrieval Model (LPRM) (Owe et al., 2001; De Jeu and Owe, 2003), Multi-Temporal Dual Channel Algorithm (MT-DCA), Multi-angular algorithm (SMOS standard algorithm)(Kerr et al. 2012; Al Bitar et al. 2017), Constrained Multi-Channel Algorithm(CMCA) (Ebtehaj and Bras, 2019; Gao et al., 2020; Konings et al., 2016), Multi-Channel Collaborative Algorithm (MCCA) (Zhao et al., 2021) were used to calculate effective optical depth and soil moisture from the *τ-ω* inverse *model.*

Accordingly, the main goals of this study are:

-Calculating effective (theoretical) optical depth, by the high order model (Tor Vergata University model) and validating the results with measured parameters (LAI, VWC and biomass) during wheat growing season.

-Calculating effective (Equivalent) optical depth using fitting method by a way these two parameters were polarization, incident angle, and frequency dependent during wheat planting to harvesting.

-Comparing the effective results with equivalent values to understand whether fitting method retrievals changes are the same as physical method retrieval changes or not.

2. Materials and Methods

2.1 Study area

Wheat canopy data were obtained at the Institute National de Recherches Agronomiques (INRA) test site in summer 1993. Measurements get from Day of Year (DOY) 90 (shortly after seeding) to DOY 175 (before harvest). They were recorded for leaf length, leaf width and thickness, stalk diameter and length; canopy height; stalk length; stalk and leaf moisture; soil and plant temperature; leaf inclination angle; density; and volumetric soil moisture (SMC). Leaf Area Index (LAI), fresh and dry biomass and VWC also were recorded. Detailed and more field data information is in Ferrazzoli et al. (Ferrazzoli et al. 2000). Multi-Frequency Microwave Radiometer (PORTOS) was used to measure the passive microwave signal or brightness temperature (TB) of wheat. It has six different frequency antennae with dual-polarized (V/H) observations. The calm water surfaces were used to do regular calibration with radiometer absolute accuracy in 3 K. Table 1 showed input variables to the models.

https://doi.org/10.5194/isprs-annals-X-4-W8-2025-765-2026

	Wheat Parameter	Unit	Min.	Max.
Leaf	Radius	cm	0.2	0.56
	Thickness	mm	0.017	0.02
	Gravimetric Moisture	%	0.66	0.81
	Angle Distribution	degree	5	85
Stalk	Radius	cm	0.108	0.22
	Length	cm	3.57	76.3
	Gravimetric Moisture	%	0.66	0.84
	Angle Distribution	degree	0	0
Layer	Mean Stalk Density	m^2	80	600
	Layer Height	m	0. 16	99

Table 1. Wheat input data for the Tor Vergata model

2.2 Optical depth by Tor Vergata University model

Optical depth for vegetation is used to describe attenuation properties, in fact, it is a measure of how opaque a vegetation canopy is when radiation passing through it (De Jeu et al. 2009). It is important in estimating soil moisture and can provide unique information on vegetation biomass and water content and canopy structure retrieval(Ulaby et al. 1982).

By means of forward scattering theorem, in vegetation transmissivity ($\lambda_p(\theta) = e^{-\tau_p sec\theta}$) function, τ is vegetation opacity and is given by($\tau_p(\theta) = k_{ep}(\theta)d$) where θ is observation angle from the nadir and d is canopy layer height and k_{ep} is the average vegetation extinction coefficient (Kurum et al. 2011). The effective optical calculated from the Tor Vergata University model by taking in to account multi scattering effects which were named VODs.

2.3 Equivalent optical depth by fitted τ-ω model

The rough surface models make the relationship between radiometer data and some properties of the observed surface such as soil moisture and vegetation optical depth. A simple zero-order model as the τ-ω model is useful and can obtain the observed surface properties by the simple process and straightforward (Kurum et al. 2011).

$$T_{B_{p,f}} = \left[(1-\omega_{p,f,v})(1-\gamma_{p,f,v})(1-e_{p,f}^{surf})(1+\gamma_{p,f,v})\right]T^{veg} + \left(\gamma_{p,f,v}T^{soil} - \left[(1-\omega_{p,f,v})(1-\gamma_{p,f,v})(1-e_{p,f}^{surf})\gamma_{p,f,v}\right]T^{veg}\right)e_{p,f}^{surf}$$

Equivalent scattering albedo and optical depth from a non-scattering medium with the same emissivity of dense vegetation are calculated. To retrieve the equivalent parameters, a root-mean-square minimization technique is used. First of all, the brightness temperature was simulated by the Tor Vergata university model in the following situations:

-Frequency:1.4 GHz, 2.69 GHz, 6.92 GHz and 10.45 GHz.
-Observation Angle:10°, 20°, 30°, 40° and 50° incident angle.
-Gravimetric soil moisture content: 0.05–0.35 m3/m3, intervals 0.05 m3/m3.
-Polarization: vertical and horizontal.
-Root mean square height: 0.5–1.5 cm of 0.5.
-Correlation length: 5–15 cm, intervals of 5.

Since, scattering albedo and optical depth are independent of soil moisture and roughness parameter, by simulating brightness temperature from the Tor Vergata model in different soil moisture and roughness parameters and fitting our simulation to the τ-ω model, it is possible to calculate effective vegetation parameters. The least square method (8) was used to obtain equivalent scattering albedo and equivalent optical depth simultaneously. In this study we named them EVOD and ESA respectively.

$$MIN\ \sqrt{\sum_{i=1}^{N}[\varepsilon_{TVU} - \varepsilon_0]^2} \qquad (8)$$

By this method, EVOD and ESA depend on polarization, incident angle and frequency. N is the number of available roughness parameters (in this study N=63), ε_{TVU} is the simulated total emissivity (the ratio of the simulated brightness and the ambient temperatures), and $\varepsilon_0$is the τ-ω model given in Equation 7. Here thermal equilibrium assumption between soil and vegetation was considered. The fitted τ-ω model codes are not publicly available due to ethical concerns. They can be requested from the author at [so.talebi@gmail.com].

3. Results

The Tor Vergata model simulation has been validated several times using field data for wheat (Eom and Fung, 1984; Ferrazzoli et al. 1995; Ferrazzoli and Guerriero, 1996; Ferrazzoli et al. 2000; Ferrazzoli et al. 2002). Figure 1 shows measured TB from radiometer and simulated TB from Tor Vergata model (L band, 40° incident angle).

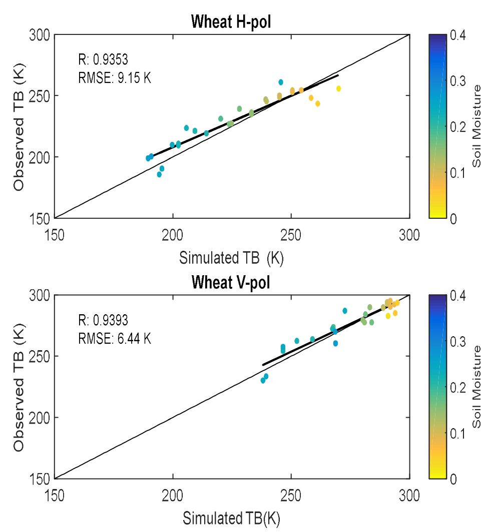

Figure 1. Comparison of radiometer measured and Tor Vergata model simulated of TB at L band in V and H pol (Talebiesfandarani et al. 2019).

It indicates the correlation coefficient between measured and simulated TB is 0.93 in V and H polarizations. The results provided an acceptable level of accuracy for the Tor Vergata model to be admitted as the theoretical basis for this study.

3.1 VODs retrievals from Tor Vergata University model:

Figure 2 indicated VODs simulation in L, S and C bands in two incident angels (10 and 50-degree) at V and H polarization. Canopy height added to the figure to compare.

The figure showed the VODs was frequency, incident angle and polarization dependent parameter. By increasing canopy height VODs increased. VODs value at 50° incident angle was higher than 10° incident angle. VODs increased by frequency because this increase leads to the decrease of penetration depth. VODs at V polarization was higher than H polarization and more incident angle dependent. VODs at H polarization at L and S bands also are incident angle dependent but because of being the same y axis in all figures, it isn't clear enough.

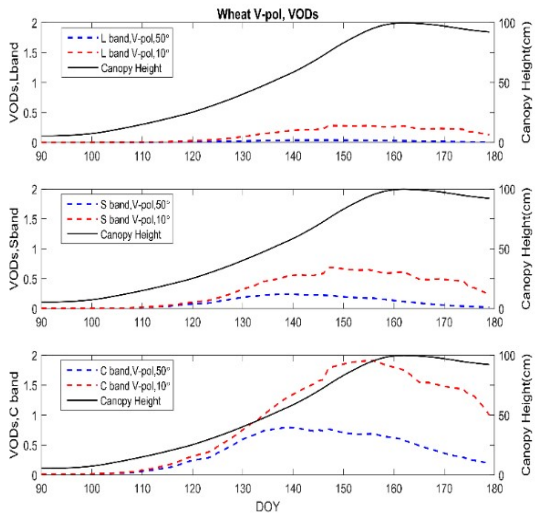

Figure 2. VODs simulation at V polarization in L, S and C bands and two incident angels (10 and 50 degree).

When vegetation optical depth was calculated correctly, it can be as an indicator of vegetation growth. Here VODs was compared with measured LAI, VWC and biomass. Figure 3 indicated that VODs were corresponding to the measured vegetation parameters according to the trend and the time of maximum and the minimum values.

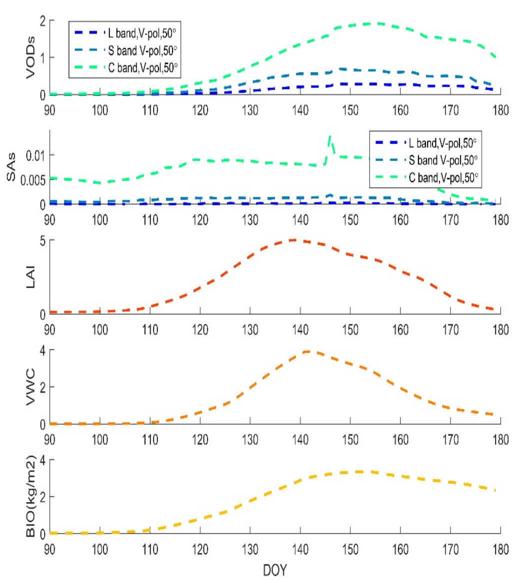

Figure 3. The trend of VODs compares to measured LAI, VWC and biomass for wheat

3.2 EVOD and ESA retrievals by fitted τ-ω model

Here, equivalent optical depth (EVOD) was calculated by fitting a high order model to zero order model to understand whether this way can work for a dense crop likes wheat or not. To obtain equivalent optical depth, brightness temperature from TVU model was simulated and fitted with the τ-ω model. Figure 4 showed the EVOD for wheat at V polarization in three bands, L, S and C. Canopy height also added to the figure to compare.

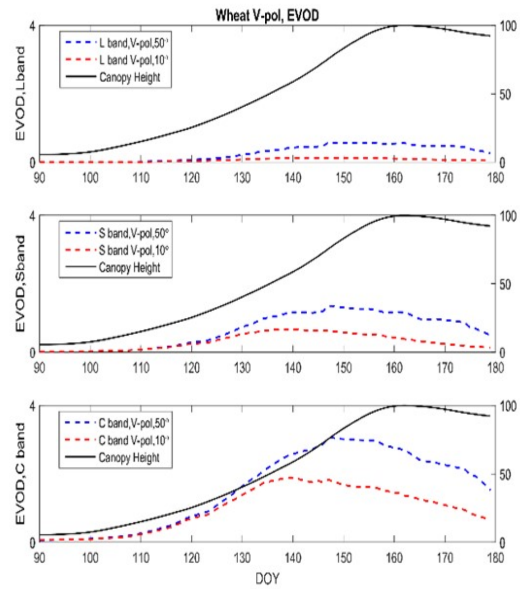

Figure 4. EVOD simulation at V and H polarization in L, S and C bands and two incident angels (10 and 50 degree).

The figure indicated that increase in canopy height leads to increase in EVOD. EVOD value at 50° incident angle was higher than 10° incident angle. Another point that should be considered is that increasing EVOD by frequency. By increasing the frequency' penetration deep was decreased and optical depth was increased. Comparing EVOD with VODs (figure 2), it was indicated although the trends of EVOD and VODs in three bands were the same, but paying attention to the EVOD values indicated little overestimated compare to VODs.

Comparing the EVOD with VODs is indicated that EVOD has acceptable correlation with VODs but is overestimated in L, S and C frequencies, H and V polarization and in 10- and 50-degree incident angles (figure 4). The smallest RMSE of the regression between VODs and EVOD occurs in L band. By increasing frequency, the RMSE increased.

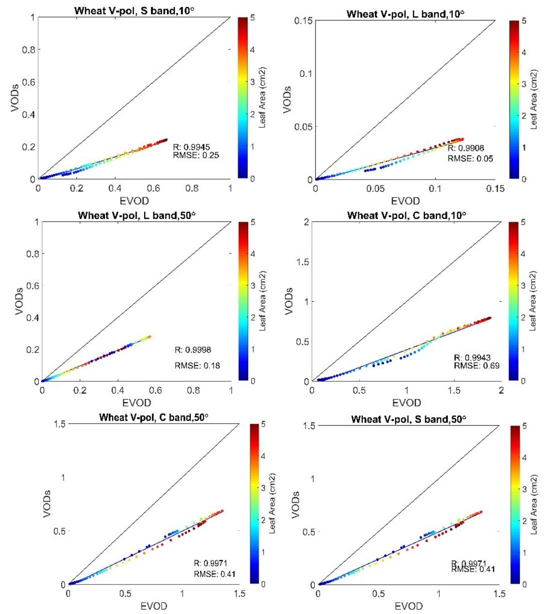

Figure 4. comparison of EVOD with VODs in L and S and C bands.

4. Discussion

The VODs was retrieved from Tor Vergata University model. The VODs depends on frequency, polarization and incident angle (Baur et al. 2019; Guangrui et al. 2021; Dou et al. 2023). By increasing canopy height, VODs increased because vegetation extinction was increased (Van de Griend and Wigneron, 2003; Hu et al. 2023; Liu et al. 2023). VODs value at 50° incident angle was higher than 10° incident angle (Wigneron et al. 2017). That's may because of longer observed vegetated canopy in 50° incident angle compare to in 10° incident angle. VODs was increased by frequency because of increasing penetration depth (Grant et al. 2016). Due to vertical structure of wheat, VODs at V polarization was higher than H polarization (Wigneron et al. 2004; Bai et al. 2018; Yao et al. 2024).

VODs was compared to the measured LAI, VWC and biomass. It was indicated that in V polarization, biomass and opacity had the best correlation with VOD(Schmidt et al. 2022).

Comparing the EVOD with VODs is indicated that lower frequencies are more suitable to calculate optical depth by fitted zero order model (like in SMAP and SMOS missions)(Schmidt et al. 2022). The least RMSE value derived for when L band in H and V polarization was applied.

Using equivalent optical depth derivation method in other types of vegetation with different structure can prepare more detail in potential of fitting method in dense vegetation.

Reference

Alemu, W. G., G. M. Henebry, 2017: "Comparing passive microwave with visible-to-near-infrared phenometrics in croplands of northern Eurasia." Remote Sensing 9(6): 613.

Asner, G. P., J. M. Scurlock, J. A Hicke, 2003: "Global synthesis of leaf area index observations: implications for ecological and remote sensing studies." Global Ecology and Biogeography 12(3): 191-205.

Au, W., L. Tsang, R. Shin, J. Kong, 1996: "Collective scattering and absorption effects in microwave interaction with vegetation canopies." Progr. Electromagn. Res 14: 181-231.

Bai, X., J. Zeng, K.-S. Chen, Z. Li, Y. Zeng, J. Wen, X. Wang, X. Dong, Z. Su, 2018: "Parameter optimization of a discrete scattering model by integration of global sensitivity analysis using SMAP active and passive observations." IEEE transactions on geoscience and remote sensing 57(2): 1084-1099.

Baur, M. J., T. Jagdhuber, A. F. Feldman, R. Akbar, D. Entekhabi, 2019: "Estimation of relative canopy absorption and scattering at L-, C-and X-bands." Remote Sensing of Environment 233: 111384.

Bracaglia, M., P. Ferrazzoli, L. Guerriero, 1995: "A fully polarimetric multiple scattering model for crops." Remote Sensing of Environment 54(3): 170-179.

Chai, L., J. Shi, L. Zhang, L. Jiang, 2010: A parameterized microwave model for short vegetation layer. 2010 IEEE International Geoscience and Remote Sensing Symposium, Ieee.

Chen, K.-S., T.-D. Wu, L. Tsang, Q. Li, J. Shi, A. K. Fung, 2003: "Emission of rough surfaces calculated by the integral equation method with comparison to three-dimensional moment method simulations." IEEE Transactions on Geoscience and Remote Sensing 41(1): 90-101.

De Jeu, R. A., T. R. Holmes, G. Van der Werf, 2009: Towards the development of a 30-year record of remotely sensed vegetation optical depth. SPIE Europe Remote Sensing, International Society for Optics and Photonics.

Dou, Y., F. Tian, J.-P. Wigneron, T. Tagesson, J. Du, M. Brandt, Y. Liu, L. Zou, J. S. Kimball, R. Fensholt, 2023: "Reliability of using vegetation optical depth for estimating decadal and interannual carbon dynamics." Remote Sensing of Environment 285: 113390.

Eom, H., A. Fung, 1984: "A scatter model for vegetation up to Ku-band." Remote Sensing of Environment 15(3): 185-200.

Ferrazzoli, P., L. Guerriero, 1996: "Passive microwave remote sensing of forests: A model investigation." Geoscience and Remote Sensing, IEEE Transactions on 34(2): 433-443.

Ferrazzoli, P., L. Guerriero, 1996: "Passive microwave remote sensing of forests: A model investigation." IEEE Transactions on Geoscience and Remote Sensing 34(2): 433-443.

Ferrazzoli, P., L. Guerriero, S. Paloscia, P. Pampaloni, 1995: "Modeling X and Ka band emission from leafy vegetation." Journal of Electromagnetic Waves and Applications 9(3): 393-406.

Ferrazzoli, P., L. Guerriero, J.-P. Wigneron, 2002: "Simulating L-band emission of forests in view of future satellite applications." IEEE Transactions on Geoscience and Remote Sensing 40(12): 2700-2708.

Ferrazzoli, P., J.-P. Wigneron, L. Guerriero, A. Chanzy, 2000: "Multifrequency emission of wheat: Modeling and applications." IEEE Transactions on Geoscience and Remote Sensing 38(6): 2598-2607.

Gao, L., M. Sadeghi, A. Ebtehaj, 2020: "Microwave retrievals of soil moisture and vegetation optical depth with improved resolution using a combined constrained inversion algorithm:

Application for SMAP satellite." Remote Sensing of Environment 239: 111662.

Grant, J., J.-P. Wigneron, R. De Jeu, H. Lawrence, A. Mialon, P. Richaume, A. Al Bitar, M. Drusch, M. Van Marle, Y. Kerr, 2016: "Comparison of SMOS and AMSR-E vegetation optical depth to four MODIS-based vegetation indices." Remote Sensing of Environment 172: 87-100.

Guan, K., A. Wolf, D. Medvigy, K. K. Caylor, M. Pan, E. F. J. E. Wood, 2013: "Seasonal coupling of canopy structure and function in African tropical forests and its environmental controls." 4(3): 1-21.

Guan, K., E. F. Wood, D. Medvigy, J. Kimball, M. Pan, K. K. Caylor, J. Sheffield, X. Xu, M. O. J. J. o. G. R. B. Jones, 2014: "Terrestrial hydrological controls on land surface phenology of African savannas and woodlands." 119(8): 1652-1669.

Guangrui, W., L. Xiaofeng, C. Xiuxue, J. Tao, Z. Xingming, W. Yanlin, W. Xiangkun, W. Jian, 2021: "An investigation on microwave transmissivity at frequencies of 18.7 and 36.5 GHz for diverse forest types during snow season." International Journal of Digital Earth 14(10): 1354-1379.

Gupta, V., N. Sharma, R. Jangid, 2013: "Emission and scattering behaviour of bare and vegetative soil surfaces of different moist states by microwave remote sensing."

Hu, L., T. Zhao, W. Ju, Z. Peng, J. Shi, N. J. Rodríguez-Fernández, J.-P. Wigneron, M. H. Cosh, K. Yang, H. Lu, 2023: "A twenty-year dataset of soil moisture and vegetation optical depth from AMSR-E/2 measurements using the multi-channel collaborative algorithm." Remote Sensing of Environment 292: 113595.

Huete, A. R., 1988: "A soil-adjusted vegetation index (SAVI)." Remote sensing of environment 25(3): 295-309.

Jackson, T. J., 1993: "III. Measuring surface soil moisture using passive microwave remote sensing." Hydrological processes 7(2): 139-152.

Jones, M. O., L. A. Jones, J. S. Kimball, K. C. J. R. S. o. E. McDonald, 2011: "Satellite passive microwave remote sensing for monitoring global land surface phenology." 115(4): 1102-1114.

Karam, M. A., A. K. Fung, Y. M. Antar, 1988: "Electromagnetic wave scattering from some vegetation samples." IEEE Transactions on Geoscience and Remote Sensing 26(6): 799-808.

Karthikeyan, L., M. Pan, A. G. Konings, M. Piles, R. Fernandez-Moran, D. N. Kumar, E. F. Wood, 2019: "Simultaneous retrieval of global scale Vegetation Optical Depth, surface roughness, and soil moisture using X-band AMSR-E observations." Remote Sensing of Environment 234: 111473.

Kerr, Y. H., P. Waldteufel, P. Richaume, J. P. Wigneron, P. Ferrazzoli, A. Mahmoodi, A. Al Bitar, F. Cabot, C. Gruhier, S. E. Juglea, 2012: "The SMOS soil moisture retrieval algorithm." IEEE transactions on geoscience and remote sensing 50(5): 1384-1403.

Konings, A. G., M. Piles, N. Das, D. Entekhabi, 2017: "L-band vegetation optical depth and effective scattering albedo estimation from SMAP." Remote Sensing of Environment 198: 460-470.

Konings, A. G., M. Piles, K. Rötzer, K. A. McColl, S. K. Chan, D. Entekhabi, 2016: "Vegetation optical depth and scattering albedo retrieval using time series of dual-polarized L-band radiometer observations." Remote sensing of environment 172: 178-189.

Kurum, M., 2013: "Quantifying scattering albedo in microwave emission of vegetated terrain." Remote Sensing of Environment 129: 66-74.

Kurum, M., R. H. Lang, P. E. O'Neill, A. T. Joseph, T. J. Jackson, M. H. Cosh, 2011: "A first-order radiative transfer model for microwave radiometry of forest canopies at L-band." IEEE Transactions on Geoscience and Remote Sensing 49(9): 3167-3179.

LeVine, D., R. Meneghini, R. Lang, S. Seker, 1983: "Scattering from arbitrarily oriented dielectric disks in the physical optics regime." JOSA 73(10): 1255-1262.

Liu, X., J.-P. Wigneron, W. Wagner, F. Frappart, L. Fan, M. Vreugdenhil, N. Baghdadi, M. Zribi, T. Jagdhuber, S. Tao, 2023: "A new global C-band vegetation optical depth product from ASCAT: Description, evaluation, and inter-comparison." Remote Sensing of Environment 299: 113850.

Liu, Y. Y., R. A. de Jeu, M. F. McCabe, J. P. Evans, A. I. J. G. R. L. van Dijk, 2011: "Global long-term passive microwave satellite-based retrievals of vegetation optical depth." 38(18).

Mätzler, C., 1994: "Microwave transmissivity of a forest canopy: Experiments made with a beech." Remote sensing of environment 48(2): 172-180.

Mo, T., B. Choudhury, T. Schmugge, J. Wang, T. Jackson, 1982: "A model for microwave emission from vegetation-covered fields." Journal of Geophysical Research: Oceans 87(C13): 11229-11237.

Njoku, E. G., P. Ashcroft, T. K. Chan, L. Li, 2005: "Global survey and statistics of radio-frequency interference in AMSR-E land observations." IEEE Transactions on Geoscience and Remote Sensing 43(5): 938-947.

O'Neill, P., R. Bindlish, S. Chan, E. Njoku, T. Jackson, 2018: "Algorithm theoretical basis document. Level 2 & 3 soil moisture (passive) data products."

Owe, M., R. de Jeu, J. Walker, 2001: "A methodology for surface soil moisture and vegetation optical depth retrieval using the microwave polarization difference index." IEEE Transactions on Geoscience and Remote Sensing 39(8): 1643-1654.

Schmidt, L., M. Forkel, R.-M. Zotta, S. Scherrer, W. A. Dorigo, A. Kuhn-Régnier, R. van der Schalie, M. Yebra, 2022: "Assessing the sensitivity of multi-frequency passive microwave vegetation optical depth to vegetation properties." Biogeosciences Discussions 2022: 1-24.

Shi, J., T. Jackson, J. Tao, J. Du, R. Bindlish, L. Lu, K. Chen, 2008: "Microwave vegetation indices for short vegetation covers from satellite passive microwave sensor AMSR-E." Remote sensing of environment 112(12): 4285-4300.

Talebiesfandarani, S., T. Zhao, J. Shi, P. Ferrazzoli, J.-P. Wigneron, M. Zamani, P. Pani, 2019: "Microwave vegetation index from multi-angular observations and its application in vegetation properties retrieval: Theoretical modelling." Remote Sensing 11(6): 730.

Tsang, L., J. A. Kong, R. T. Shin, 1985: Theory of microwave remote sensing, Wiley New York.

Ulaby, F., R. Moore, A. Fung, 1982: "Microwave remote sensing: Active and passive. Volume 2-Radar remote sensing and surface scattering and emission theory."

Ulaby, F., R. Moore, A. Fung, 1986: "Microwave Remote Sensing: Active, Passive vol III: From Theory to Applications (Dedham, MA: Artech House)."

Ulaby, F. T., F. Kouyate, B. Brisco, T. L. Williams, 1986: "Textural infornation in SAR images." IEEE Transactions on Geoscience and Remote Sensing(2): 235-245.

Ulaby, F. T., D. G. Long, W. J. Blackwell, C. Elachi, A. K. Fung, C. Ruf, K. Sarabandi, H. A. Zebker, J. Van Zyl, 2014: Microwave radar and radiometric remote sensing, University of Michigan Press Ann Arbor.

Van de Griend, A. A., J.-P. Wigneron, 2003: "Canopy extinction and single scattering albedo in the microwave region as a function of frequency, polarization, incidence angle and canopy type." IEEE Transactions on Geoscience and Remote Sensing.

Wigneron, J.-P., A. Chanzy, J.-C. Calvet, N. Bruguier, 1995: "A simple algorithm to retrieve soil moisture and vegetation biomass using passive microwave measurements over crop fields." Remote Sensing of Environment 51(3): 331-341.

Wigneron, J.-P., T. Jackson, P. O'Neill, G. De Lannoy, P. De Rosnay, J. Walker, P. Ferrazzoli, V. Mironov, S. Bircher, J. Grant, 2017: "Modelling the passive microwave signature from land surfaces: A review of recent results and application to the L-band SMOS & SMAP soil moisture retrieval algorithms." Remote Sensing of Environment 192: 238-262.

Wigneron, J.-P., M. Pardé, P. Waldteufel, A. Chanzy, Y. Kerr, S. Schmidl, N. Skou, 2004: "Characterizing the dependence of vegetation model parameters on crop structure, incidence angle, and polarization at L-band." IEEE Transactions on Geoscience and Remote Sensing 42(2): 416-425.

Yao, Y., V. Humphrey, A. G. Konings, Y. Wang, Y. Yin, N. Holtzman, J. D. Wood, Y. Bar-On, C. Frankenberg, 2024: "Investigating diurnal and seasonal cycles of Vegetation Optical Depth retrieved from GNSS signals in a broadleaf forest." Geophysical Research Letters 51(6): e2023GL107121.

Zhao, T., J. Shi, D. Entekhabi, T. J. Jackson, L. Hu, Z. Peng, P. Yao, S. Li, C. S. Kang, 2021: "Retrievals of soil moisture and vegetation optical depth using a multi-channel collaborative algorithm." Remote Sensing of Environment 257: 112321.

This contribution has been peer-reviewed. The double-blind peer-review was conducted on the basis of the full paper.
https://doi.org/10.5194/isprs-annals-X-4-W8-2025-765-2026 | © Author(s) 2026. CC BY 4.0 License.